GEOPHYSICAL RESEARCH LETTERS, VOL. 27, NO. 6, PAGES 775-778, MARCH 15, 2000

Recent Changes in Arctic Ocean Sea Ice Motion Associated with the North Atlantic Oscillation

Ronald Kwok

Jet Propulsion Laboratory, California Institute of Technology, Pasadena, California

Abstract. Examination of a new ice motion dataset of the Arctic Ocean over a recent eighteen year period (1978-1996) reveals patterns of variability that can be linked directly to the North Atlantic Oscillation. The intensity of the Icelandic Low, one of its centers of action, modulates the sea level pressure distribution over a broad region of the Arctic Ocean and the Greenland-Iceland-Norwegian and Barents Seas. Over the winters of 1988 through 1995, the Oscillation has remained in its positive phase contributing to coherent large-scale changes in the intensity and character of ice transport in the Arctic Ocean. The significant changes include: the weakening of the Beaufort Gyre; the increase in ice export through the Fram Strait; the increase in ice import from the Barents/Kara Seas; the enhanced eastward transport of sea ice from the Laptev Sea; the weakening of the Transpolar Drift Stream; and, the reduction in ice extent in the Nordic Seas. All of these changes affect the regional and total sea ice mass balance of the Arctic Ocean.

1. Introduction

The North Atlantic Oscillation (NAO) is a major source of interannual variability in the atmospheric circulation pattern in the winter North Atlantic. It accounts for more than one-third of the total variance in the sea-level pressure (SLP). *Hurrell* [1995] defined an index of the NAO based on the difference of normalized SLP between Lisbon, Portugal and Stykkisholmur, Iceland. The positive phase of NAO (NAO+) is characterized by an intense Icelandic low with a strong Azores ridge to its south. This low affects a broad region of the Arctic Ocean. The signs of these anomalies are reversed in its negative phase (NAO-). There was a prolonged period of NAO+ since 1988 followed by a dramatic reversal in phase in 1996 (Fig. 1). Between 1978 and 1987, there are approximately an equal number of months (37 vs 40) with NAO < -1 and NAO > 1. After 1987, there were 40 months with NAO > 1 and only 21 months with NAO < -1.

Through wind forcing, these changes in the SLP distributions over the Arctic Ocean have significant impact on the patterns of sea ice circulation. Away from coastal boundaries, the geostrophic wind explains more than 70% of the variance of daily ice motion in both winter and summer [*Thorndike and Colony*, 1982]. This large-scale circulation of sea ice determines the advective part of the ice balance and changes in the circulation pattern affects ice export, ice extent and regional mass balance. The present paper examines changes in the Arctic Ocean sea ice motion associated with the NAO using a new 18-year ice motion data set derived from satellite passive microwave imagery and buoy data. The observed changes in the ice motion pattern, ice flux, and ice extent are discussed.

Copyright 2000 by the American Geophysical Union.

Paper number 1999GL002382.
0094-8276/00/1999GL002382$05.00

2. Ice Motion Data Set

A number of studies [*Agnew et al.*, 1997; *Liu and Cavalieri*, 1998; *Kwok et al.*, 1998] have recently been demonstrated that ice motion can be derived from sequential satellite passive microwave imagery. The fairly coarse spatial resolution of the imagery produces standard deviations of about 6 km for individual displacement vectors. The great strengths of this data set are its spatial coverage and the length of the data record that is nearly twenty years for the combination of SMMR (Scanning Multifrequency Microwave Radiometer) and SSM/I (Special Sensor Microwave Imager). The ice motion data set used here are created by combining ice motion estimates from satellite brightness temperature fields (37 GHz, 85 GHz) and buoy drift into 2-day motion fields, viz.,

$$\hat{u} = \sum_i \alpha_i u_i^{85GHz} + \sum_j \beta_j u_j^{37GHz} + \sum_k \gamma_k u_k^{buoy}$$

where u is ice motion and α, β and γ are weighting coefficients determined by an optimal interpolation procedure [*Colony and Thorndike*, 1984]. The buoy data are obtained from International Arctic Buoy Program (IABP). The output motion fields are sampled on a 100 km by 100 km grid. Based on the number of observations used and errors in the passive microwave ice motion fields and the buoy drifts, the procedure above provides an analysis of the error of each motion estimate. Here, it gives an expected average uncertainty of 1-2 km/day in the interpolated estimates.

3. Results and Discussion

We compiled composites of the monthly fields of SLP (from IABP) and ice motion based on monthly NAO indices

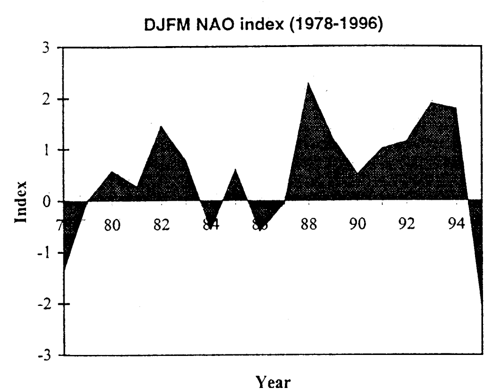

Figure 1. Winter (December through March) index of the NAO based on the difference of the normalized pressure between Lisbon, Portugal and Stykkisholmur, Iceland (after *Hurrell* (1)). The DJFM NAO indices are averages of their monthly values.

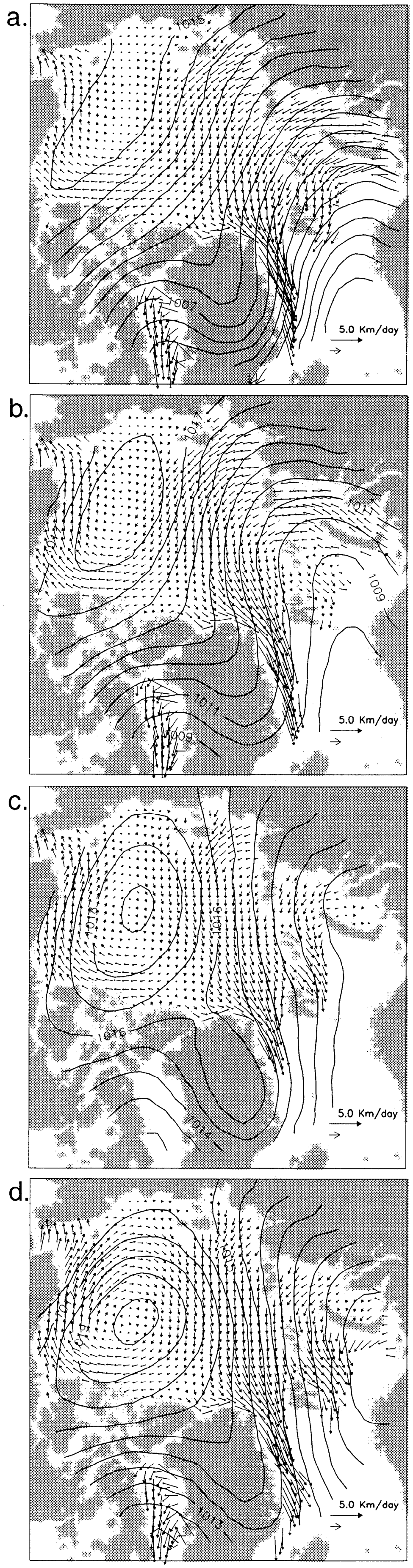

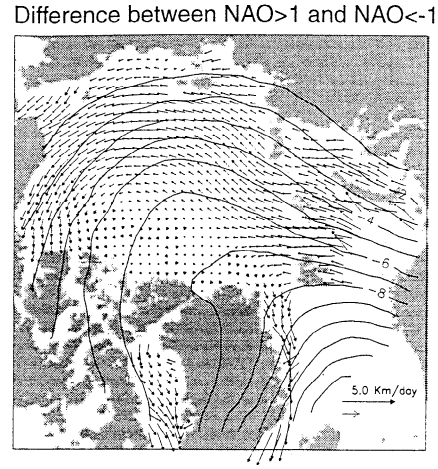

Figure 3. Difference between the NAO > 1 (Fig. 2a) and NAO ≤ -1 (Fig. 2d) sea-level pressure and ice motion fields.

(Fig. 2). These fields show distinct shifts in spatial patterns that are associated with opposing phases of NAO (Fig. 2). The difference field (Fig. 3) shows how the intense Icelandic Low in the positive phase imparts an enhanced cyclonic component on atmospheric circulation and sea ice motion. In the immediate area of the Icelandic Low, the composite difference exceeds 12 hPa. During NAO-, there is a well-defined high pressure cell centered over the Beaufort Sea. By contrast, there are no closed isobars over the Arctic Ocean during NAO+. Poleward of 70°N, the extremes of SLP are smaller during NAO- (range: 1020-1008 hPa) than during NAO+ (range: 1015-998 hPa) even though the surface pressure over the central Arctic is much higher. *Walsh et al.* [1996] first noted a weakening of the Arctic anticyclone since 1988, most likely due to the dominance of the Icelandic Low during the prevailing NAO+ conditions in the late 1980s and early 1990s. The SLP variations over the Arctic Ocean (shown in Figs. 2 and 3) are also captured in the Arctic Oscillation [*Thompson and Wallace*, 1999]. Strengthening of the polar vortex is associated with lower surface pressure. The mean SLP in the central Arctic decreased by almost 5 hPa over the 18-year period between 1978-1995. The Eurasian Low pressure cell centered over the Barents Sea during NAO- is situated further southwest under NAO+ conditions. Intermediate SLP distributions are evident between the two NAO extremes.

Changes in the circulation patterns related to the NAO affect ice flux, ice extent, ice age and thickness distributions in the Arctic Ocean. During NAO-, the Beaufort Gyre (anticyclonic sea ice circulation in the Canada Basin) and the Transpolar Drift Stream (TDS) are distinctive features in the mean motion fields (1978-1987) associated with the Beaufort high pressure cell centered within the Canada Basin and the Icelandic Low. The TDS transports sea ice from the north of Siberia and the Beaufort Sea toward Fram Strait. All four fields (in Fig. 2) show flow out of the Laptev Sea, a primary

Figure 2. Composite patterns of monthly (October through May) sea-level pressure and ice motion fields between 1978 and 1996 partitioned based on the monthly NAO index. (a) NAO > 1. (b) 0 < NAO ≤ 1. (c) -1 < NAO ≤ 0. (d) NAO ≤ -1. The contour increment is 1 hPa.

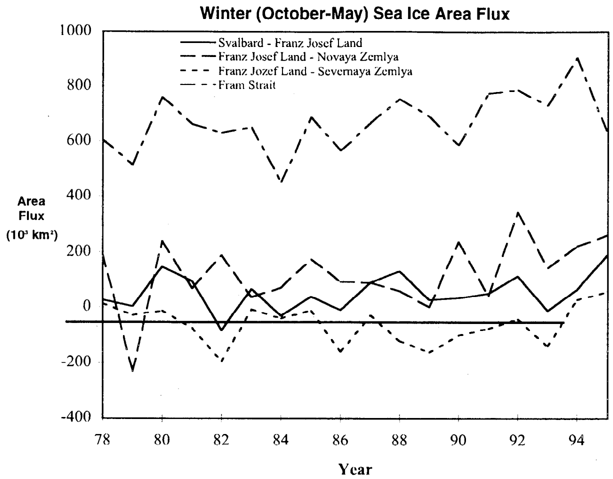

Figure 4. Time series of ice area flux through Fram Strait (after *Kwok and Rothrock*, 1999), Svalbard-Franz Josef Land, Franz Josef Land-Novaya Zemlya, Franz Josef Land - Severnaya Zemlya.

source of ice in the TDS. In contrast, the Beaufort Gyre is not fully formed in the NAO+ motion fields and the TDS has a different character. There is no significant flow parallel to the Siberian coast in the East Siberian Sea. Ice from the Laptev and the Kara is advected further east before being entrained in a weakened TDS with its axis shifted westward toward the Canada Basin due to the enhanced cyclonic Icelandic Low. *Steele and Boyd* [1998] suggest that this is associated with the transport of more fresh riverine shelf water from the Kara and Laptev further east before such water flows out into the deep basins, leading to the retreat of cold halocline layer from the Amundsen into the Makarov Basin in the 1990s. The circulation patterns in the NAO+ and NAO- extremes are not unlike the two regimes of wind-forced ice circulation discussed *in Proshutinsky and Johnson* [1997].

Kwok and Rothrock [1999] report significant correlation (R =0.86, significance level ~10^{-4}) between the sea ice area flux through Fram Strait and the NAO index over the months of December through March (Fig. 4). They showed an upward trend in the areal flux associated with the positive phase of NAO. The areal flux varied by a factor of 1.6 over the last 18 years. Correlations are reduced during the negative NAO years because of the decrease in the cross-strait pressure gradient. The Fram Strait fresh water flux, transported by sea ice and low salinity water, may affect the global thermohaline circulation: a key element of the climate system on decadal to millennial time-scales [*Broeker et al.*, 1985]. Modeling studies suggest that if this circulation is disrupted or weakened the consequences for high-and mid-latitude continental climate could be severe [*Manabe and Stouffer*, 1988]. Small changes in Fram Strait outflow are thought to affect the delicate density stratification in the Greenland, Iceland, and Norwegian Seas and are sufficient to permit or restrain deep convection. Correlation between five years of volume flux estimates (1991-1995) and the NAO index, admittedly a small sample size, gives R=0.56. The average winter volume flux over the winters of Oct 1990 through May 1995 is 1745 km^3. It ranges from a low of 1375 km^3 in 1991 to a high of 2791 km^3 in 1995, varying by a factor of two over the short five year record of NAO+. With this magnitude of variability, the excess fresh water of 2000 km^3 first observed north of Iceland during the mid-1960s characterized as the 'Great Salinity Anomaly' [*Dickson et al.*, 1988] can therefore be accounted for by only moderate perturbations of outflow from the Arctic Ocean [*Aagaard and Carmack*, 1989].

Lower correlations between the volume flux and the NAO (relative to the area flux) is likely because volume flux is dependent on the ice thickness of the source regions in addition to the variability in atmospheric forcing. Due to changes in the TDS, the outflow through Fram Strait (see Fig. 2) comes from quite different parts of the Arctic Ocean under different NAO conditions. This suggests that the variability of NAO affects the mean thickness of the ice outflow, regional mass balance and total ice volume of the Arctic Ocean. The regional outflow rate determines the residence time and in turn the regional ice age and ice thickness. The NAO+ motion fields seem to favor source regions in the Eurasian Basin whereas the NAO- motion fields indicate larger contributions of sea ice from the East Siberian Sea and thicker ice from the Beaufort Sea. South of Fram Strait, the ice motion fields also show enhanced transport through the Denmark Strait due to increased pressure gradient associated with NAO+ (Table 2).

The Kara Sea appears to be a net exporter of sea ice, sometimes into the eastern Arctic Ocean and other times into the Barents Sea. The area flux of sea ice (1978-1996) through the following passages: Svalbard-Franz Josef Land, Franz Jozef Land-Novaya Zemlya and Franz Josef Land-Severnaya Zemlya are shown in Fig. 4. The ice area flux through these passages are small compared to the Fram Strait outflow and all are negatively correlated, although not all significantly, to the NAO index (Table 1). The strength of the correlation is most likely dependent on the orientation of the passages relative to the cyclonic circulation pattern due to the Icelandic Low. The most significant volume exchange is the inflow sea ice from the Barents and Kara Seas through the Franz Josef Land-Severnaya Zemlya passage. There was sustained inflow of sea ice through this passage during the prevailing NAO+ conditions between 1988-1996.

The sea ice extent in the Greenland and Barents Seas is also linked to the NAO. The time series of April ice extent anomalies from satellite passive microwave observations exhibits a downtrend over the eighteen years and is negatively correlated (-0.64, significance~0.003) with the DJFM NAO index. The southerly winds under the cyclonic circulation pattern tend to advect the ice edge northward and westward. This is consistent with the ice motion pattern in these regions (Table 2). During NAO+, the zonal component of ice motion in the East Greenland Sea is toward the Greenland coast thus decreasing the ice extent. The meridional component, however, is enhanced as indicated by the increase in ice area flux discussed above. Under NAO- conditions, the zonal component of ice motion is much higher, transporting the ice southward and eastward toward the Greenland Sea. In contrast, the meridional component of ice motion in the

Table 1. Arctic Ocean area flux ($10^3 km^2$) October through May 1978 - 1996. ('+' indicates outflow)

Flux Gate	Avg	Min	Year	Max	Year	Correlation/Significance (NAO/Area Flux)
Svalbard - Franz Josef Land	47	-83	1982	187	1995	-0.52/0.025
Franz Josef Land - Novaya Zemlya	126	-232	1979	348	1992	-0.17/0.49
Franz Josef Land - Severnaya Zemlya	-65	-195	1982	52	1995	-0.74/0.001

Table 2. Partitioning of meridional (v_m) and zonal (v_z) ice velocities (cm/s) based on NAO index

Location (lat, lon)		1 < NAO		0 < NAO < 1		-1 < NAO < 0		NAO < -1	
		v_m	v_z	v_m	v_z	v_m	v_z	v_m	v_z
a) East Greenland Sea									
69N	20W	-6.0	-4.7	-6.9	-2.2	-5.0	-0.2	-5.3	-2.4
72N	16W	-8.3	-3.0	-8.7	-2.5	-6.9	-1.4	-6.5	-0.4
75N	12W	-10.1	-1.5	10.5	-2.2	-9.5	0.1	-7.3	0.6
b) Barents Sea									
78N	35E	-0.2	-3.0	-1.4	-0.8	-2.1	-3.1	-3.2	-2.5
78N	40E	0.0	-3.2	-1.7	-1.1	-2.1	-3.4	-3.1	-2.8
78N	45E	0.8	-2.8	0.6	-0.7	-1.4	-3.2	-2.7	-3.4
78N	50E	1.7	-2.4	0.2	-0.3	-1.0	-2.9	-1.4	-3.5
c) Baffin Bay/Davis Strait									
69N	60W	-8.7	2.7	-8.5	0.9	-5.3	-0.3	-6.5	0.6
72N	64W	-5.0	2.4	-5.5	3.0	-4.4	0.3	-4.1	1.0
73N	68W	-4.7	3.2	-4.9	2.8	-4.1	1.2	-3.9	2.1

Barents Sea is much higher during low NAO. This favors the southward motion of the ice edge increasing ice coverage in the Barents Sea. The NAO+ motion fields also show enhanced southward advection of sea ice in Baffin Bay and Davis Strait (Table 2). Large positive sea ice extent anomalies and negative surface air temperature anomalies in Hudson Bay, Baffin Bay and Labrador Sea during episodes of strong NAO were reported by *Rogers and van Loon* [1979] and *Mysak et al.* [1996].

4. Summary Remarks

The present paper examines the linkages between the recent changes in the Arctic Ocean ice motion, ice flux, and ice extent and the NAO using an 18-year ice motion data set derived from satellite and buoy observations. The composite plots in Fig. 2 show the coherent changes in the large scale ice circulation associated with progressive changes in the NAO index. During the prolonged period of NAO+ since 1988, the ice circulation and SLP patterns of Figs. 2a and 2b dominate while Figs. 2c and 2d are the prevailing patterns during NAO- conditions. The Icelandic Low, the northern center of action of the NAO, affects the SLP over a broad region of the Arctic Ocean and thus the pattern of sea ice circulation. Most significant are the correlations of ice area and volume flux in the 1990s and the NAO index. Within the Arctic Ocean, the effects of shifts in ice circulation pattern on regional mass balance remain to be modeled. Other studies [*Zhang et al.*, 1998; *Dickson et al.,* 1999] have reported increased moisture flux into the Arctic, increased ocean transport into the Arctic Ocean through the Barents Sea, and a warming and freshening of Atlantic Water inflow to the Arctic Ocean in the West Spitzbergen Current, all in connection with the positive phase of the NAO (North Atlantic Oscillation) index since the late 1980s. Our contribution adds to this growing body of evidence of recent changes in the Arctic Ocean and their connections to the North Atlantic Oscillation.

Acknowledgments. I wish to thank J. C. Comiso for providing the time-series of ice extent of the Greenland and Barents Seas. The sea level pressure and buoy drift data are provided by the International Arctic Buoy Program. This work was performed at the Jet Propulsion Laboratory, California Institute of Technology, and was sponsored by the National Aeronautics and Space Administration and the National Oceanic and Atmospheric Administration.

References

Aagaard, K., and E. Carmack, The role of sea ice and other fresh water in the Arctic circulation, *J. Geophys. Res. 94*(C10), 14,485-14,498, 1989.

Agnew, L., H. Le, and T. Hirose, Estimtion of large scale sea ice motion from SSM/I 85.5 GHz imagery, *Ann. Glacio*., 25, 305-311, 1997.

Broecker, W. S., D. M. Peteet and D. Rind, Does the ocean-atmosphere system have more than one stable mode? *Nature*, 315, 21-26, 1985.

Colony, R. and A. Thorndike, An estimate of the mean field of Arctic sea ice motion, *J. Geophys. Res* , 89(C6), 10623-10629, 1984.

Dickson, R. R., J. Meincke, S. Malmberg, and A. J. Lee, The "Great Salinity Anomaly" in the Northern Atlantic, *Prog. Oceanog.*, 20, 103-151, 1988.

Dickson, R. R., T. J. Osborn, J. W. Hurrell, J. Meincke, J. Blindheim, B. Adlandsvik, T. Vinje, G. Alekseev, W. Maslowski and H. Cattle, The Arctic Ocean response to the North Atlantic Oscillation, , *J. Clim.*, in press.

Hurrell, J. W. Decadal trends in the North Atlantic Oscillation: regional temperatures and precipitation, *Science*, 269, 676-679, 1995.

Kwok, R., A. Schweiger, D. A. Rothrock, S. Pang and C. Kottmeier, Sea ice motion from satellite passive micrwave data assessed with ERS and buoy motions, *J. Geophy. Res.*, 103(C4), 8191-8214, 1998.

Kwok, R. and D. A. Rothrock, Variability of Fram Strait ice flux and North Atlantic Oscillation, *J. Geophy. Res.*, 104, 5177 (1999).

Liu, A. and D. J. Cavalieri, On sea ice drift from the wavelet analysis of DMSP SSM/I data, *Int. J. Remote Sens*., 19(7), 1415-1423, 1998.

Mysak, L. A., R. G. Ingram, J. Wang and A. van der Baaren, The anomalous sea-ice extent in Hudson Bay, Baffin Bay and the Labrador Sea during three simultaneous NAO and ENSO episodes, *Atmosphere-Ocean*, 35, 333 (1996).

Proshutinsky, A. Y. and M. A. Johnson, Two circulation regimes of the wind-driven Arctic Ocean, *J. Geophy. Res.*, 102, 12,493-12,514, 1997.

Rogers, J. C. and H. van Loon, The seesaw in winter temperatures between Greenland and northern Europe. Part II: Some oceanic and atmospheric effects in middle and high latitudes, *Mon. Wea. Rev*., 107, 509-519.

Steele, M. and S. Boyd, Retreat of the cold halocline layer in the Arctic Ocean, *J. Geophy. Res.*, 103, 10419 (1998).

Thompson, D. W. J. and J. M. Wallace, The Arctic Oscillation signature in the wintertime geopotential height and temperature grids, *Geophys. Res. Lett*., in press.

Thorndike, A. and R. Colony, Sea ice motion in response to geostrophic winds, *J. Geophy. Res*., 87, 5845 (1982).

Walsh, J. E., W. L . Chapman and T. L. Shy, Recent decrease of sea-level pressure in the Central Arctic, *J. Clim*., 9, 480-486, 1996.

Manabe, S. and R. J. Stouffer, Two stable equilibria of a coupled ocean atmosphere model, *J. Clim*., 841-866, 1988.

Zhang, J., D. A. Rothrock and M. Steele, Warming of the Arctic Ocean by a strengthened Atlantic inflow: Model Results, *Geophy. Res. Lett*., 25, 1745 (1998).

R. Kwok, Jet Propulsion Laboratory, California Institute of Technology. 4800 Oak Grove Drive, Pasadena, CA 91109. (e-mail: Ron.Kwok@jpl.nasa.gov)

(Received July 26, 1999; revised October 15, 1999; accepted January 14, 2000.)